Bollettino di Geofisica Teorica ed Applicata Vol. 52, n. 3, pp. 513-538; September 2011
DOI 10.4430/bgta0013

The contribution of the ambient vibration prospecting in seismic microzoning: an example from the area damaged by the April 6, 2009 L'Aquila (Italy) earthquake

D. Albarello[1], C. Cesi[2], V. Eulilli[2], F. Guerrini[1], E. Lunedei[1], E. Paolucci[1], D. Pileggi[1] and L.M. Puzzilli[2]

[1] *Dipartimento di Scienze della Terra, Università degli Studi, Siena, Italy*
[2] *Dipartimento Difesa del Suolo – Servizio Geofisica, ISPRA, Roma, Italy*

(Received: April 22, 2010; accepted: July 21, 2010)

ABSTRACT Ambient vibration prospecting represented an important tool for the seismic characterization of shallow geological structures in the areas damaged by the April 6, 2009 L'Aquila (Italy) earthquake. Just after the mainshock, in the first exploratory phases, single-station ambient vibration monitoring (HVSR approach) was widely applied by several research groups operating in the area to detect sites where possible resonance phenomena could had been responsible for damage enhancement. Afterwards, ambient vibration measurements both in the single-station and multi-station (seismic array) configurations were extensively applied to support seismic microzoning studies and in particular, to constrain geological reference models and local V_S profiles. The procedures adopted in these field activities are described in detail, along with both first-glance interpretations and refined inversion procedures applied in exploratory surveys and seismic microzoning activities. The parallel application of other prospecting techniques (geological surveys, resistivity prospecting, drilling, etc.) allowed us to validate the experimental procedures adopted and to define protocols useful for future applications.

Key words: seismic microzoning, geophysical prospecting, ambient vibrations, L'Aquila earthquake.

1. Introduction

On April 6, 2009 a seismic event (M_W = 6.3) hit the Abruzzo region, in central Italy. Although it was not a very strong earthquake, it caused serious damage in the city of L'Aquila and in most parts of the surrounding municipalities: some villages were completely destroyed, more than a thousand people were injured and more than 300 of them died. Just after the event, several groups of researchers and professional geologists and engineers, coordinated by the University of Basilicata on the behalf of the Dipartimento della Protezione Civile (National Department of Civil Protection - DPC), carried on an extensive survey of single-station ambient vibration measurements by using the approach proposed by Nakamura (1989), also known as Horizontal-to-Vertical Spectral Ratios or HVSR approach [see SESAME (2004) and references therein]. The main goal of this survey was a preliminary identification of sites where significant amplification of the seismic ground motion, induced by stratigraphic resonance phenomena, could have been responsible for observed damage. After this exploratory phase, an extensive program of seismic microzoning studies was planned and several working groups were given the responsibility of

providing seismic microzoning maps for the municipalities damaged by the mainshock (DPC, 2009). The basic purpose was to provide local administrations with an effective tool for reconstruction plans and management of provisional structure location. This activity also aimed at the field validation of the seismic microzoning guidelines, recently published in 2009 (Gruppo di Lavoro MS, 2008), that would represent a basic tool for future anti-seismic planning.

To manage the relevant field activities, the study area was subdivided into 12 "macroareas", each including several municipalities and settlements with severe earthquake damage (DPC, 2009; Gruppo di Lavoro MS L'Aquila, 2011). For each macroarea, several geological, geophysical and geotechnical surveys were planned, that were entrusted to several institutions. More precisely, this operation involved about 150 researchers e technicians of 8 Universities (L'Aquila, Chieti-Pescara, Genova, Politecnico di Torino, Firenze, Basilicata, Roma "La Sapienza", Siena), 7 Research Institutions (CNR, INGV, AGI, RELUIS, ISPRA, ENEA, OGS), 4 Regional and Provincial Authorities (Lazio, Emilia-Romagna, Toscana, Trento) and one Professional Association (Ordine dei Geologi dell'Abruzzo).

This paper describes the application of ambient vibration monitoring carried out by the research unit of the Department of Earth Sciences of the University of Siena (hereafter UNISI) in support of the seismic microzoning of two macroareas (6 and 7), coordinated by the Istituto Superiore per la Protezione e la Ricerca Ambientale (hereafter ISPRA).

In the first part of the paper, the experimental procedures adopted in ambient vibration (or passive) prospecting will be described along with preliminary interpretation schemes and refined inversion procedures. Two prospecting configurations were considered: single station and multiple station. Single-station three-directional ambient vibration measurements have been adopted to determine the local resonance frequency, by considering the HVSR approach cited above. The multiple station approach (seismic array) was considered to determine the vertical Rayleigh wave dispersion curves and used to constrain the local V_S profile (e.g., Parolai *et al*., 2005; SESAME, 2005). In the second part of the paper, the application of these procedures in the study area is briefly outlined by focusing on methodological aspects connected to the development of effective experimental protocols to be used in future applications.

2. Single-station measurements (HVSR)

The basic goal of single-station measurements is the determination of the fundamental resonance frequency of the soft sedimentary cover (SESAME, 2004). To this purpose, average ratios (H/V) of horizontal (H) to vertical (V) spectral components of ambient vibrations are measured in the field. Despite the fact that physical interpretation of the H/V ratios as a function of frequency (hereafter HVSR curve) is to some extent controversial (Nakamura, 2000; Fäh *et al*., 2001; Lunedei and Albarello, 2010), the frequency f_0 corresponding to the maximum value of the H/V function was shown to have a strict correspondence with the local resonance frequency f_r of the sedimentary cover (see, e.g., Bonnefoy-Claudet *et al*., 2006). By exploiting the well known approximate relationships relating the resonance frequency of this cover with its thickness (h) and average S-wave velocity ($\langle V_S \rangle$),

$$h \simeq \frac{\langle V_S \rangle}{4 f_0} \tag{1}$$

(see, e.g., Ibs Von Seht and Wohlemberg, 1999), one can see that f_0 deduced from HVSR measurements allows us to retrieve important information on the shallow subsoil structure.

Experimental determination of H/V curves was performed by a three-directional digital tromograph Tromino Micromed (see www.tromino.it) with a sampling frequency of 128 Hz and an acquisition time of 20 minutes, by following the procedure described in Picozzi *et al*. (2005) and D'Amico *et al*. (2008). Maxima inside the frequency range of engineering interest [0.5, 20] Hz were taken into account only.

Before a geological/geophysical interpretation is attempted, the quality of HVSR curves were evaluated in agreement with international consensus criteria (see SESAME, 2004). According to these, first curve reliability (i.e., suffcient number of windows and significant cycles for a given f_0, acceptably low scattering among all windows over a given frequency range around f_0) was verified. Then, reliability of HVSR peaks (i.e., fulfillment of amplitude and stability criteria) was checked. Particular attention was devoted to the identification of eventual peaks induced by low-frequency disturbances (wind blowing, in case of near tall buildings, bad soil-sensor coupling, etc.) and to better resolve broad or multiple peaks (i.e., by varying the smoothing parameters).

In order to provide an immediate indication about the quality of single measurements and preventing over-interpretation of bad experimental results, a classification scheme to rank HVSR measurements was developed, in agreement with other groups operating in the area. Since this classification includes a larger number of elements, it turns out to be more conservative than that proposed by the SESAME group (SESAME, 2004). Three classes were defined:

- *class A*: trustworthy and interpretable HVSR curve, which represents a reference measurement that can be considered representative of the dynamical behavior of the subsoil at the site of concern by itself;
- *class B*: suspicious HVSR curve, which should be used with caution and only if it is coherent with other measurements performed nearby;
- *class C*: bad HVSR curve (it is hardly interpretable), to be discarded.

Criteria used to classify a single measurement as of class A are:

i. stationarity: HVSR curve included in the frequency range of interest shows a persistent shape for at least the 30% of the measurement windows;
ii. isotropy: the azimuthal amplitude variations do not exceed 30% of the maximum;
iii. absence of artifacts: there are not symptoms of electromagnetic noise or peaks of industrial origin into the frequency range of interest;
iv. physical plausibility: HVSR maxima are characterized by a localized lowering of the vertical amplitude spectral component;
v. statistical robustness: SESAME criteria for a reliable H/V curve are fulfilled;
vi. representative sampling: the measurement took place for at least 15 minutes.

A measurement is in class B if one or more of the previous conditions are not fulfilled. Measurements of class B become of class C if:

- a rising drift exists from low to high frequencies, that indicates a movement of the

instrument during the acquisition (Forbriger, 2006), or
- electromagnetic disturbances affect several frequencies in the frequency range of interest.

Actually, these criteria aimed at the "first-glance" identification of good and unreliable measurements (A and C classes respectively) and at identifying doubtful results (B class), that require careful inspections. These criteria did not concern the possibility to provide a physical interpretation of the curve in terms of "absence/presence" of resonance phenomena. For this purpose, the SESAME conditions for "peak clearness" were taken into account. On this basis, two sub-classes (type) were introduced:
- *type 1:* the HVSR curve presents at least one clear peak in the frequency range of interest (possible resonance);
- *type 2:* the HVSR curve does not present any clear peak in the frequency range of interest (absence of resonance).

In order to set up a complete database of survey results, each single-station measurement was accompanied by a report including photos of the measuring site and the SESAME Measurement Field Sheet (SESAME, 2004), where the operator recorded information relative to field conditions (spatio-temporal localization, progressive acquisition number, ground and weather conditions, building density, possible noise sources, nearby structures, pedestrian and vehicular traffic and other situations that potentially can affect the measurement). The report also includes the most important outcomes of the processing procedure (HVSR curve, relative power components, directional and time analysis, check of SESAME criteria) along with relevant class and type by following criteria reported above.

3. Multi-station measurements (seismic arrays)

Multi-station measurements were also carried out. This technique consists in recording ambient vibration ground motion by means of an array of sensors (geophones) distributed at the surface of the subsoil to be explored (see, e.g., Okada, 2003). Relevant information concerning phase velocities of waves propagating across the array are obtained from average cross-spectral matrixes relative to sensor pairs. In the present analysis, plane waves propagating across the array were considered only. Since only vertical sensors were used, these waves are interpreted as plane Rayleigh waves in their fundamental and higher propagation modes.

Determination of Rayleigh wave phase velocities V_R as a function of frequency (dispersion curve) was obtained from cross-spectral matrixes by the Extended Spatial AutoCorrelation (ESAC) technique (Ohori *et al*., 2002; Okada, 2003) in the form proposed by Parolai *et al*. (2006). This technique, provides a unique V_R curve, defined as the "effective" Rayleigh wave dispersion curve. In the case that the vertical component of ambient vibrations were mainly constituted by Rayleigh waves in their fundamental propagation mode, V_R strictly corresponds to the Rayleigh wave dispersion curve. However, in the case that several propagation modes exist, this becomes an "effective (or apparent)" dispersion curve, that is a combination of the dispersion curves relative to the relevant modal components (Tokimatsu, 1997). The fact that the ESAC approach allows the determination of the apparent dispersion curve instead of the modal ones could represent an important limitation of this procedure with respect to other approaches (e.g., *f–k* techniques). On the other hand, this makes the approach here considered more robust with

respect to the alternative procedures, since it does not require troublesome picking of existing propagation modes.

In the present study, ambient vibrations were recorded for 20 minutes at a 128 Hz sampling rate by using 16 vertical geophones (4.5 Hz) and a digital acquisition system BrainSpy produced by Micromed. Geophones were placed along two crossing perpendicular branches (with maximum dimensions lower than 100 m) and irregularly spaced (in the range 0.5÷30 m). Using the ESAC technique, wavelengths even higher than 2÷3 times the largest inter-geophonic distance can be monitored (Okada, 2003). Because maximum depth of investigation is about 1/2÷1/3 of the largest wavelength analyzed, the adopted array configuration allowed us to reach depths of up to 100 m approximately.

4. Inversion of ambient vibration measurements

The basic feature of ambient vibration measurements is providing a fast and cheap prospecting tool, useful to supply information for seismic microzoning. In this regard, the detection and the characterization of resonance phenomena induced by the trapping of seismic energy within soft sedimentary covers overlying a rigid seismic bedrock (resonant layers) is of major importance. In particular, resonance frequency f_r is of great concern. Since it roughly depends on the ratio between the average S-wave velocity in the soft layer and the thickness of this last one, the direct f_r estimates provided by HVSR (f_0) contribute to constrain the thickness of the sedimentary cover when some information about the local V_S profile is available. To this purpose, Rayleigh wave dispersion curves deduced from array measurements can be of concern since they allow us to constrain the seismic velocity profile (see, e.g., Xia *et al*., 1999; Parolai *et al*., 2006). Thus, the joint use of single-station and multi-station ambient vibration measurements could provide an important contribution to the development of a reliable geological model of the area of interest and to feed numerical procedures devoted to the assessment of seismic response.

However, the possibility of using HVSR and dispersion curves for this purpose is limited by the complex relationship that exists between the relevant parameters (V_S profile, depth of the seismic bedrock, etc.) and observables such as $V_R(f)$ and f_0 (see, e.g., Arai and Tokimatsu, 2004, 2005; Lunedei and Albarello, 2009, 2010; Albarello and Lunedei, 2010). Thus, numerical inversion procedures have to be applied to retrieve relevant parameters from observations (see, e.g., Menke, 1989; Sambridge and Mosegaard, 2002). These procedures have to manage the strong non-linearity of the inverse problem that makes the results obtained largely non-univocal. Furthermore, these become numerically troublesome and highly time consuming. Thus, for field interpretation of experimental curves, some "fast and dirty" procedures were applied in the cases under examination, to supply at least a preliminary interpretation of collected data. A basic limitation of these procedures is the use of very simplified models and the separate interpretation of HVSR and dispersion curves. The main advantage is the quickness and the numerical simplicity that permit their use in the field just after the measurement has been taken. Afterwards, more advanced inversion procedures were applied to better constrain the local structural models. In particular, a genetic algorithm approach (Yamanaka and Ishida, 1996) was considered on purpose.

4.1. "Fast and dirty" inversion procedures

The basic hypothesis underlying these procedures is that Rayleigh waves in the fundamental mode dominate ambient vibration wavefield. A second assumption is that these waves propagate within a nearly homogeneous soft layer (characterized by V_S values smoothly increasing with depth) overlying a rigid bedrock. In particular, one assumes a V_S profile in the form

$$V_S(z) \simeq V_0 \cdot (1+z)^x, \tag{2}$$

which holds for each dimensionless $z \geq 0$: $V_S(z)$ is the S-wave velocity as a function of the depth $(1+z) \cdot 1$ m, V_0 is the S-wave velocity at 1 m under the ground surface and $x \in]0, 1[$ is a suitable exponent (see Appendix). In this assumption, it is possible (Ibs Von Seht and Wohlemberg, 1999) to establish a simple approximate relationship between the resonance frequency f_r and the thickness of the soft sedimentary layer h:

$$h \simeq \left[\frac{V_0(1-x)}{4 f_r} + 1 \right]^{\frac{1}{1-x}} - 1. \tag{3}$$

Since $f_0 \cong f_r$, Eqs. (1) and (3) make it also possible to evaluate the average $\langle V_S \rangle$ velocity up to the seismic bedrock via equation

$$\langle V_S \rangle \simeq 4 f_0 h \simeq 4 f_0 \left\{ \left[\frac{V_0(1-x)}{4 f_0} + 1 \right]^{\frac{1}{1-x}} - 1 \right\}. \tag{4}$$

This method requires at least a rough definition of the free parameters V_0 and x. Some indications about possible realistic values for these parameters are shown in the Appendix. More specialized values can be provided by a preliminary geological survey or by considering borehole data eventually available (e.g., D'Amico *et al.*, 2004, 2008). Otherwise, this information can be provided by a direct interpretation of available effective Rayleigh wave dispersion curves, that, in the frame of the approximation considered above, coincides with the fundamental Rayleigh mode. In this case, several authors (Konno and Kataoka, 2000; Martin and Diehl, 2004; Albarello and Gargani, 2010) suggested, on the basis of empirical evidence, that the average S-wave velocity up to a depth of h roughly corresponds to the Rayleigh waves phase velocity relative to a fixed wavelength of the order of $1 \div 3$ times h. As an example, by defining for each frequency f the couple $\lambda \equiv V_R(f)/f$ and $v(\lambda) \equiv V_R(f)$, Martin and Diehl (2004) suggested $\langle V_S \rangle_{30\,\mathrm{m}} \equiv 1.045 \cdot v(\lambda_0)$, with $\lambda_0 \equiv 40$ m. By generalizing, the average S-wave velocity at depth h is assumed to roughly correspond to Rayleigh wave velocity according to:

$$\langle V_S \rangle_h \simeq V_R(f) \quad with \quad h \simeq (0.3 \div 0.5) \cdot \frac{V_R(f)}{f}. \tag{5}$$

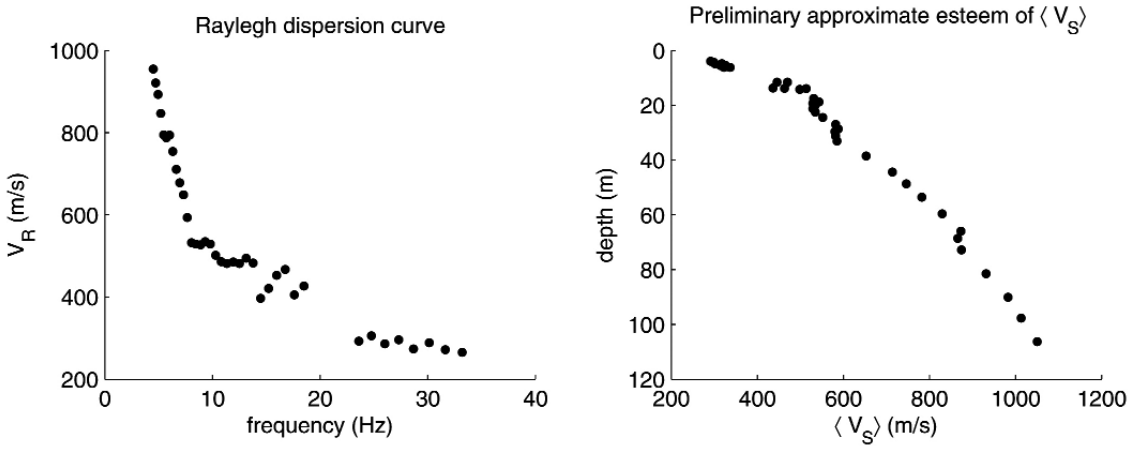

Fig. 1 - Example of "fast and dirty" inversion by dispersion curve at site of Pedicciano. Left: experimental V_R curve. Right: approximate pattern of average S-wave velocity profile obtained by Eq. (6).

This implies that the effective dispersion curve deduced from array measurements could be used directly to constrain V_0 and x values. In particular, V_R values relative to highest frequencies can be considered as a rough estimate of V_0, while x can be estimated from the literature (see Appendix), or by best fitting the $\langle V_S \rangle_h$ curve. In order to obtain a first-glance information on the S-wave velocity profile (in particular to establish the depth of the main impedance contrasts and the approximate variability range of the S-wave velocities), we made use of the approximate relationship:

$$\left\langle V_S \right\rangle_h \equiv 1.1 \cdot V_R(f) \quad with \quad h \equiv \frac{V_R(f)}{2f}. \tag{6}$$

Fig. 1 shown the application of Eq. (6) to the dispersion curve obtained from the array in one of our studied sites in the Abruzzo region.

4.2. Refined joint inversion procedure

Advanced numerical inversion procedure were used to retrieve more reliable parameterization of the local V_S profile. To this purpose, joint inversion of HVSR and V_R curves was performed.

In general, different inversion procedures exist, belonging to two families whose end-members are local-search and global-search ones. Methods in the first group start form a guess solution, and evolve it by subsequent linear approximations (linearized methods). Since they only explore the solution space near the guess solution, their feasibility strongly depends on the guess solution itself, which needs to be close to the exact one in order to make the procedure converge. On the other hand, global methods are more robust since they do not require starting solutions (but as concerns the overall limits of the search hypervolume) and explore the whole parameter space. Nevertheless, linear methods converge very quickly if the starting solution is near enough

the true one, while global ones are very time consuming. Hybrid methods also exist that merge the two approaches (Picozzi and Albarello, 2007). In the present study, since poor a priori information was available in advance (see above), a global-search inversion procedure was considered. In particular, the genetic algorithm method (see, e.g., Yamanaka and Ishida, 1996) was adopted. This is basically a Monte Carlo method, which is able to explore the whole parameter space (set of layer velocities, densities and quality factors). Nevertheless the research procedure is not uniformly random on the parameter space, but it is driven by an "evolutional" mechanism that, as the research is going on, concentrates exploration in the more promising areas. In this sense it is a hybrid approach between local and global search algorithm.

A genetic algorithm is an iterative procedure, consisting in a sequence of steps. *In primis* a set of models (seismic velocity profiles, etc.) is generated by means of a random criterion: it is the first generation. The second step is an allotment of a score to each model, according to its fit, i.e., inversely to its misfit function value: this is a measure of the distance between the experimental curves (HVSR and V_R as function of the frequency in the present case) and the ones produced by the theoretical model via the forward simulation code. Afterwards, a new generation is created by applying the genetic operators: cross-over, mutation and elite selection. The first operator generates a number (usually two) of new profiles by crossing, via a random rule, the variables of two original profiles, chosen proportionally to their score. The mutation changes some values of the new profile, according to a specific mutation probability. The last operator selects a number of best models, which directly transit in the new generation. All these procedures are governed by random runs, based on some probability *a priori* sets. The procedure repeats on until a specific condition is fulfilled (minimum misfit value or maximum generation number). In this way, the best model is obtained by mimicking the natural evolution. It is worth noting that, in this procedure, it is essential to set an appropriate parameter search space, i.e., a range of variability for each parameter, as, e.g., thickness and S-wave velocity of each stratum. To make realistic this setting, we made use of all the available information: minimum and maximum V_R value, HVSR peaks, approximate depths given by Eq. (3), approximate average S-wave velocity given by Eq. (6), available geological maps, electrical tomographies. As the work was proceeding, and as new geological and geophysical information became available, the inversions were repeated to include new pieces of information.

An important aspect of inversion is the forward modeling implemented in the procedure. In the present case, we assumed the subsoil as a flat stratified viscoelastic medium where surface waves (Rayleigh and Love with relevant higher modes) propagate only (Lunedei and Albarello, 2009). From this model, both theoretical HVSR and effective dispersion curves can be computed from a set of parameters representative of the hypothetical subsoil (V_S, V_P, density, Q_P and Q_S profiles). The discrepancy between theoretical and observed HVSR and dispersion curves were then evaluated in terms of a suitable misfit function, strictly linked to the well-known χ^2 function, and that allowed different choices about the combination of the discrepancies of V_R and HVSR curves, with different weights as well.

Results of this inversion procedure have the form shown by the example in Fig. 2.

5. Field application in the April 6, 2009 L'Aquila earthquake

Under the coordination of ISPRA, the UNISI research group was charged to support, with

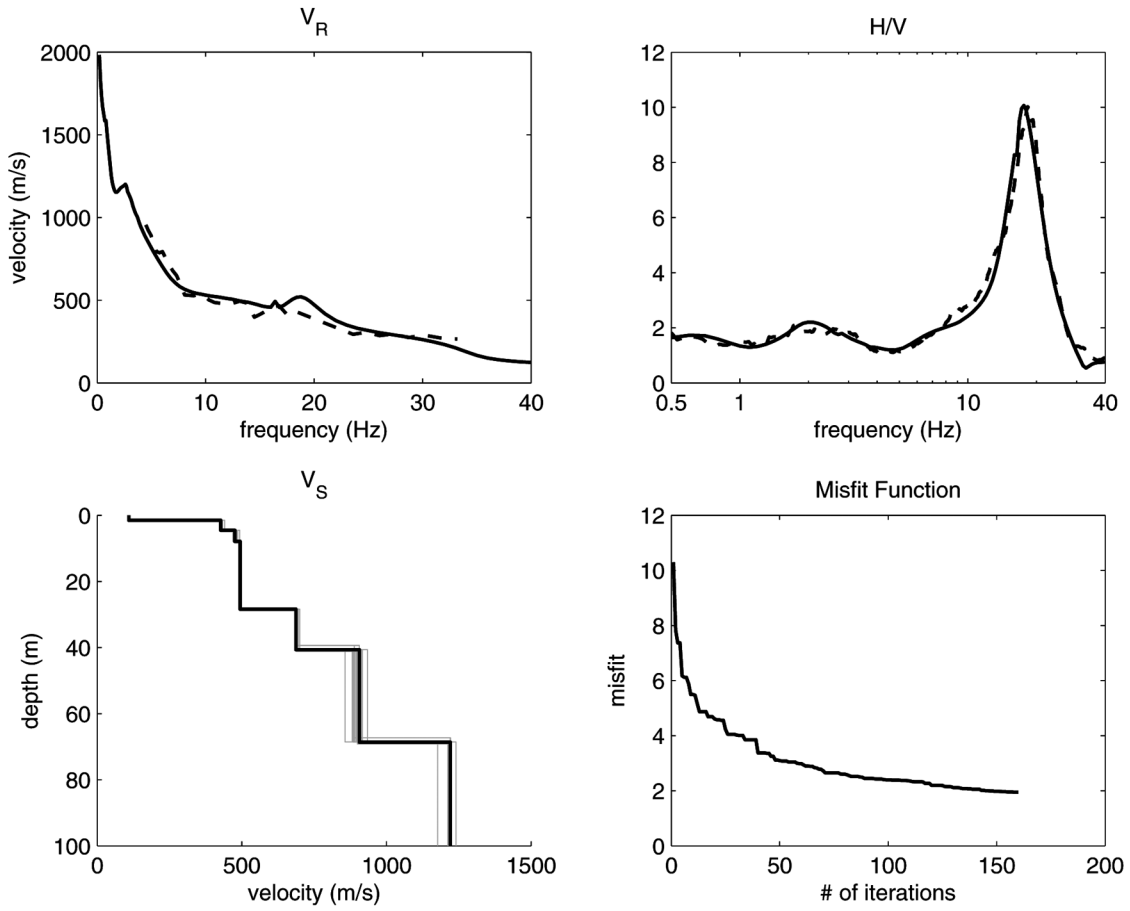

Fig. 2 - Example of joint inversion results of the effective dispersion curve (V_R) and the HVSR curve for the site of Pedicciano. Top left: comparison of theoretical dispersion curve resulting by the inversion (solid line) and the experimental ones (dashed line). Top right: comparison of theoretical HVSR curve (solid line) and the experimental ones (dashed line). Bottom left: the S-wave velocity profile of the best-fit model (black line) with (grey lines) the velocity values of the profile with a misfit function value not higher than the 10% of the one of the best-fit model. Bottom right: the best misfit function pattern.

ambient vibration measurements, the development of a reference geological model to be used for numerical simulations of the seismic response at the settlements of (see Fig. 3):

- macroarea 6: Sant'Eusanio Forconese, Casentino, Fossa, Villa Sant'Angelo, Tussillo;
- macroarea 7: Arischia, San Demetrio nei Vestini, Stiffe, Vallecupa, Pedicciano.

The first goal of the survey was providing information useful to constrain the geological model of the considered areas. This model represents the first step for the development of seismic microzoning maps (Gruppo di Lavoro MS, 2008). In this context, defining the shape of the seismic bedrock (i.e., the shallowest significant seismic impedance contrast in the subsoil) was of major importance. To this purpose and to provide estimates of representative V_S profiles (or at least of the average V_S value up to the bedrock) an extensive campaign of ambient vibration

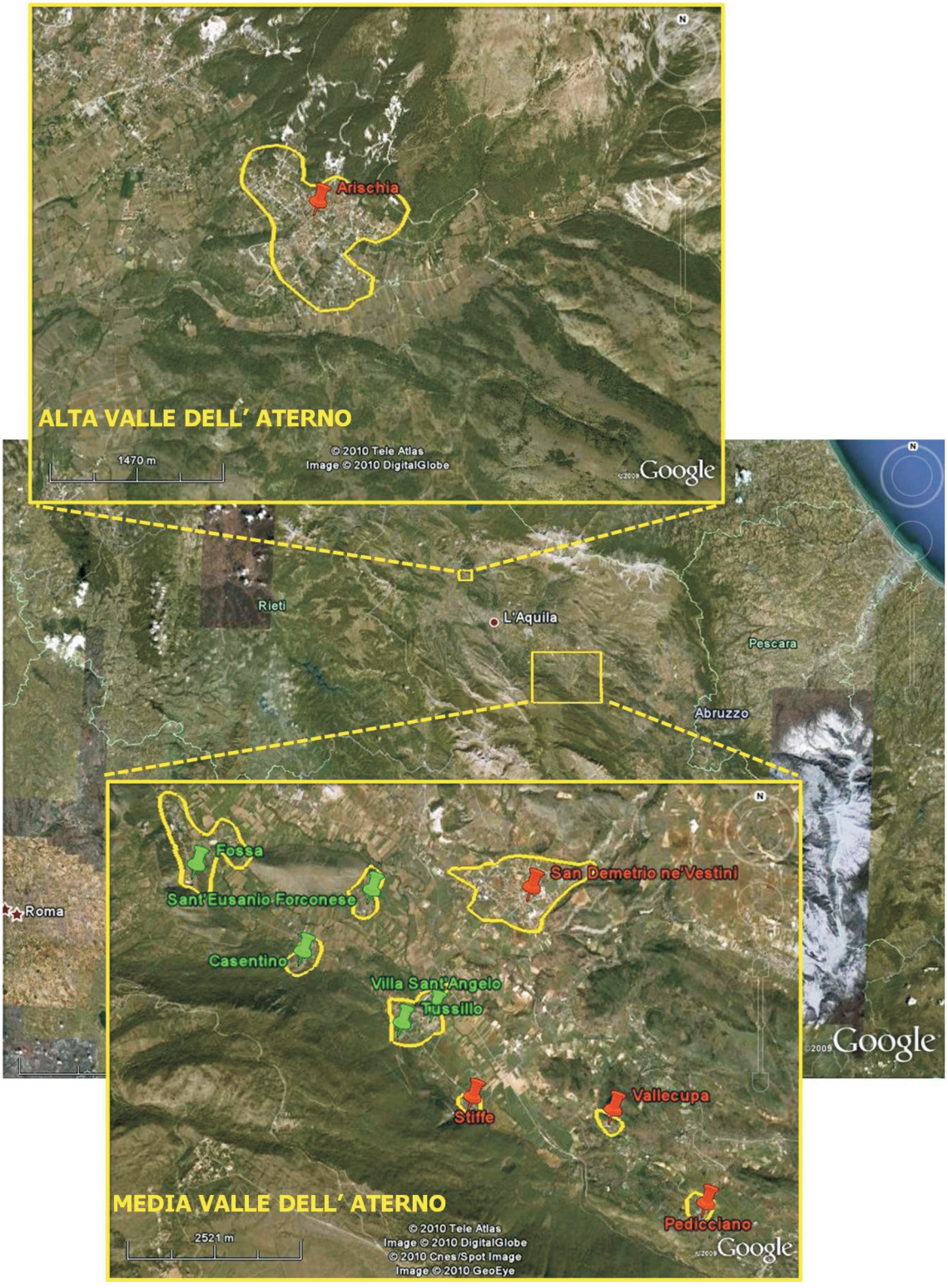

Fig. 3- Geographical localization of investigated areas.

measurements (both in single-station and multi-station configurations) was planned. More damaged areas (where population was completely evacuated) as well as their surroundings were considered in the geophysical surveys by including areas where rebuilding activities and new settlements were planned by local administrations. Measurement sites were selected in order to:

- privilege areas with major damages (so called *zone rosse)*, in the hypothesis that heavier damages could be associated to amplification effects induced by local seismic stratigraphy;
- characterize major geological bodies defined according to data provided by very preliminary large scale (1:50,000) geological surveys;
- warrant a satisfactory level of redundancy and homogeneity in the distribution of ambient vibration measurements.

As a whole, during a time span of about one week with one crew of 4 operators, single station HVSR measurements were carried out in 98 places. At 8 of these sites multi-station acquisition were also performed.

Collected data were implemented in a geographical database in the Google Earth environment. This allowed a fast and easy comparison of results provided by on-going geological surveys carried out by ISPRA.

The database includes 3 main layers above the geographic frame provided by Google Earth. The first layer hosts all the measurement points, classified according to the criteria in chapter 2. This layer allows an immediate view of the degree of coverage provided by the survey and of the overall quality of available assessments. In the second layer, details of HVSR measurements (HVSR curve and average spectra relative to the three spatial components) are reported in graphical form to allow associating and correlating HVSR results obtained in neighboring sites. Effective dispersion curves, provided by array measurements, were also reported in this layer. This allowed immediate correlation of measurements provided in nearby sites and to compare instrumental results with those provided by preliminary geological surveys, reported in the third and last layer of the database.

Thanks to this database, a further examination of the HVSR in class B was performed, and each of them have been accepted or rejected on the basis of its consistency or not with the surrounding measurements.

5.1. Interpretation of ambient vibration measurements

Just after the field work, single-station ambient vibration measurements were processed to obtain a “first glance” interpretation in support of geological surveys. This was achieved in two steps. First of all, HVSR measurements were considered to identify areas where possible seismic resonance phenomena take place. In particular, geological bodies hosting type 1 HVSR curves were enlightened. In this phase, the coherence of neighboring measurements was used to evaluate the actual reliability of class B measurements. At the sites where significant HVSR peaks were identified, a very rough estimate of the depth of the seismic bedrock was attempted on the basis of the correspondences in the Table 1, deduced from the results discussed in subsection 4.1 and in the Appendix. This piece of information was communicated to geologists involved in the field work and helped them in developing the preliminary geological model. In the following, seismic array data were analyzed and jointly inverted with HVSR curves available at the relevant sites to provide more refined V_S profiles. To this purpose, genetic algorithm inversion procedures

Table 1 - Approximate summary relationship between HVSR peak frequency (f_0) and impedance contrast depth (h), deduced by Eq. (3) and considerations in Appendix.

f_0 (Hz)	h (m)
< 1	> 100
1 ÷ 2	50 ÷ 100
2 ÷ 3	30 ÷ 50
3 ÷ 5	20 ÷ 30
5 ÷ 8	10 ÷ 20
8 ÷ 20	5 ÷ 10
> 20	< 5

(subsection 4.2) were extensively applied by retrieving eight V_S profiles down to a depth of about 50 ÷ 100 m, depending on the array length.

The availability of broadly distributed single-station measurements in the explored areas allowed to extend V_S profiles deduced at the array laterally. Where a geologically homogeneous sedimentary cover is expected, thickness of the sedimentary cover was adjusted to fit observed f_0 values by adopting V_S values determined at the array. In this way, the whole area surrounding a known profile was characterized at least as concerns gross features. This possibility is one of the main merits of the passive seismic survey, and is very important when in the zones of concern it is difficult to perform geophysical surveys requiring relatively large soil occupancy, as in the case of, e.g., historical centres or hamlets.

Other geophysical surveys were also planned in support of geological studies for the investigated area. Both direct explorations (drilling) and active seismic prospecting (down-hole, MASW, refraction seismic tests) were carried out by other work groups. These last studies provided important constraints to the local stratigraphy (by means the geological drillings) and the velocity profile of S-waves (by means of active seismic surveys). In addition, ISPRA carried out 14 resistivity surveys in the tomomographic configuration. To this purpose a resistivimeter Syscal R2 by IRIS Instruments was used with 96 electrodes spaced from 2.5 to 5 m. All these data allowed us to better constrain results provided by ambient vibration measurement and supported the geological interpretation of detected seismic impedance contrasts. Furthermore, these data also allowed us to test results provided by the preliminary analysis of ambient vibration measurements.

Figs. 4 and 5 summarize the results of the joint inversions performed, by the genetic algorithm method, in the eight above-mentioned investigated sites: they show a large variety of different subsoil configurations. In each of the considered sites, a strong main impedance contrast is highlighted, that divides the shallow soft sedimentary cover from a deeper stiff soil and it is the principal responsible of the observed resonance peak. The seismic substratum reveals very different properties depending on the site. In some cases, it may coincide with the geological bedrock (Meso-Caenozoic limestones): sites of Sant'Eusanio Forconese (a in Fig. 4), Villa Sant'Angelo (b in Fig. 4), Arischia (e in Fig. 4) and probably Pedicciano (h in Fig. 4). In case B this holds although the S-wave velocity in the substratum is lower than 800 m/s, probably depending on the rock alteration or

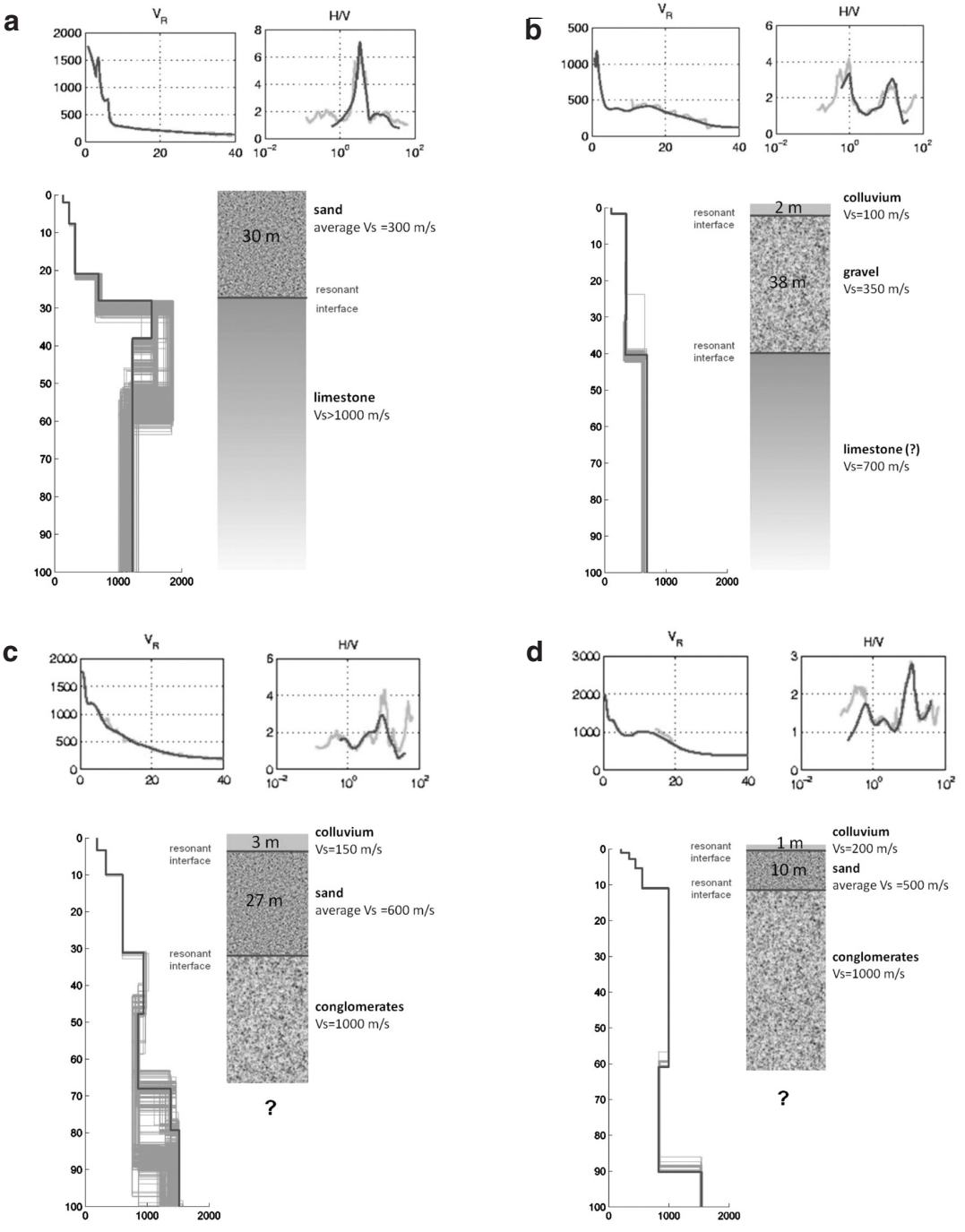

Fig. 4 - Inversion results and stratigraphic interpretation of 4 sites: a) Sant'Eusanio Forconese, b) Villa Sant'Angelo, c) San Demetrio nei Vestini (Cardamone), d) San Demetrio nei Vestini (Villagrande). For each site, dispersion curve (V_R) and HVSR curve (H/V) are shown in the upper part of the corresponding panel: grey lines are the experimental curves, black lines are the ones correpoonding to the preferred interpretative model. In the lower part of the panel, best fitting S-wave velocity profile (black line) is reported along with profiles with a misfit value not higher than the 10% of the one associated to the best-fit model (grey lines). A tentative stratigraphic interpretation of the corresponding best fitting model is also reported.

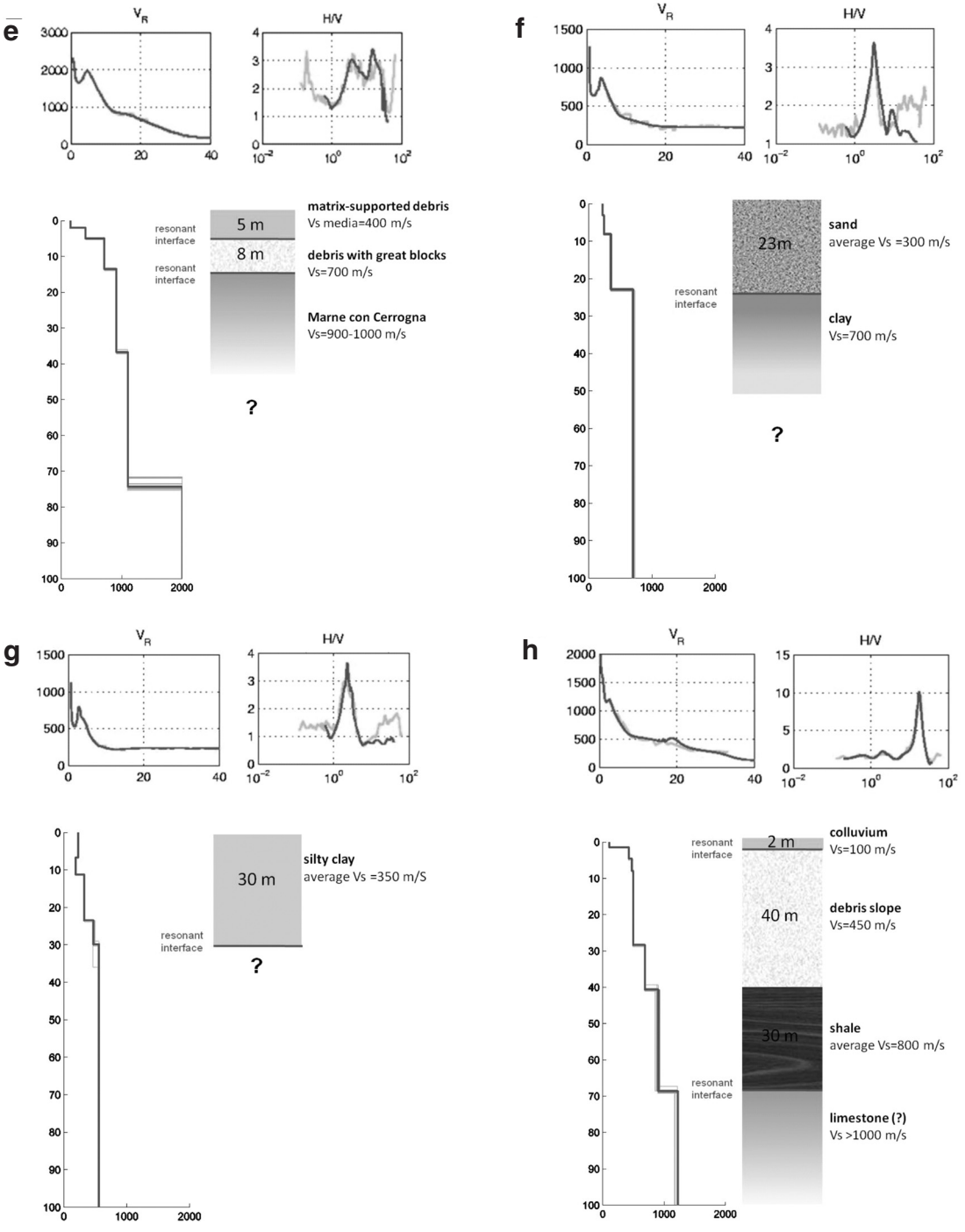

Fig. 5 - Inversion results and stratigraphic interpretation of other sites: e) Arischia, f) Stiffe, g) Vallecupa, h) Pedicciano. See caption of Fig. 4 for panel explanation.

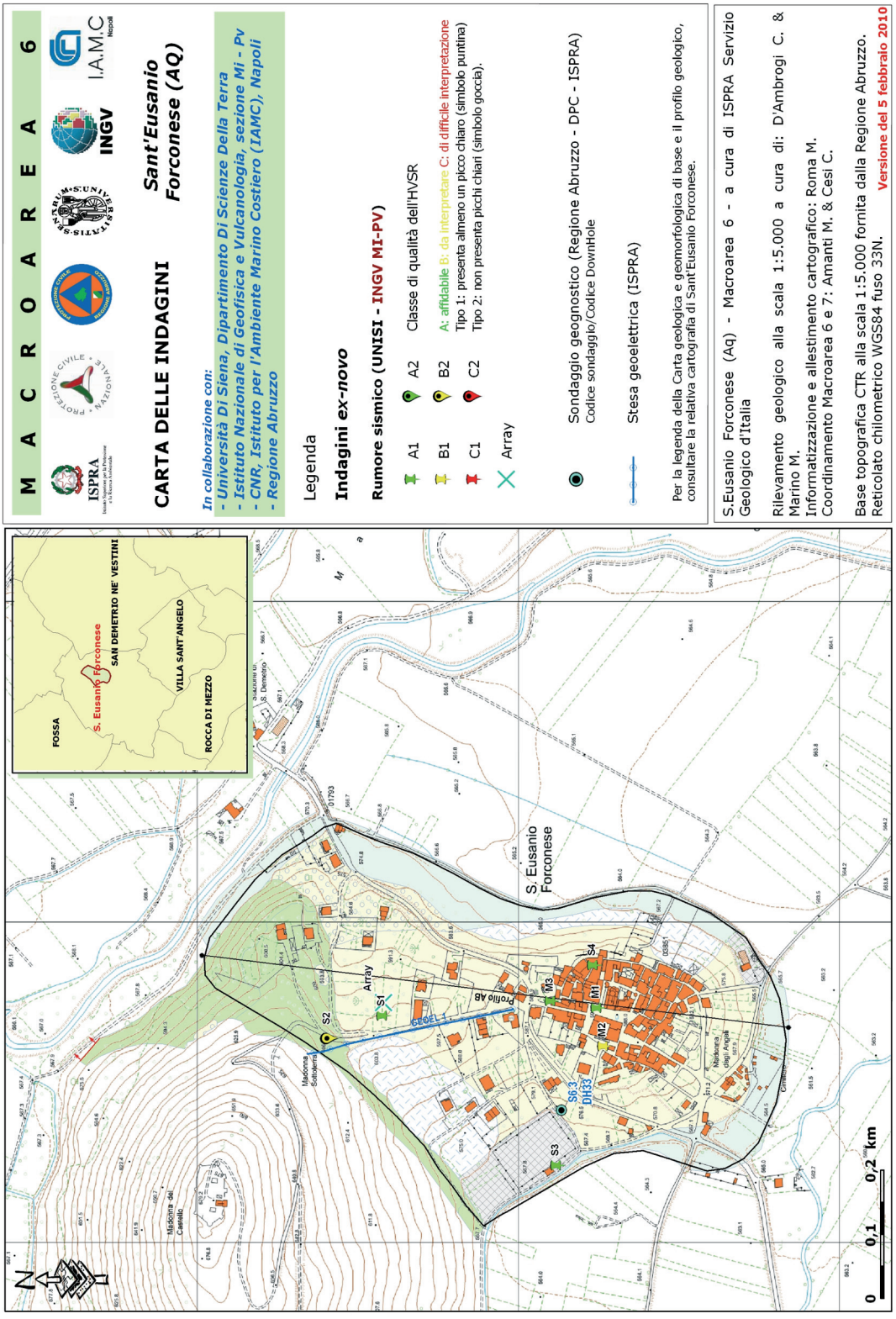

Fig. 6 - Survey map of Sant'Eusanio Forconese.

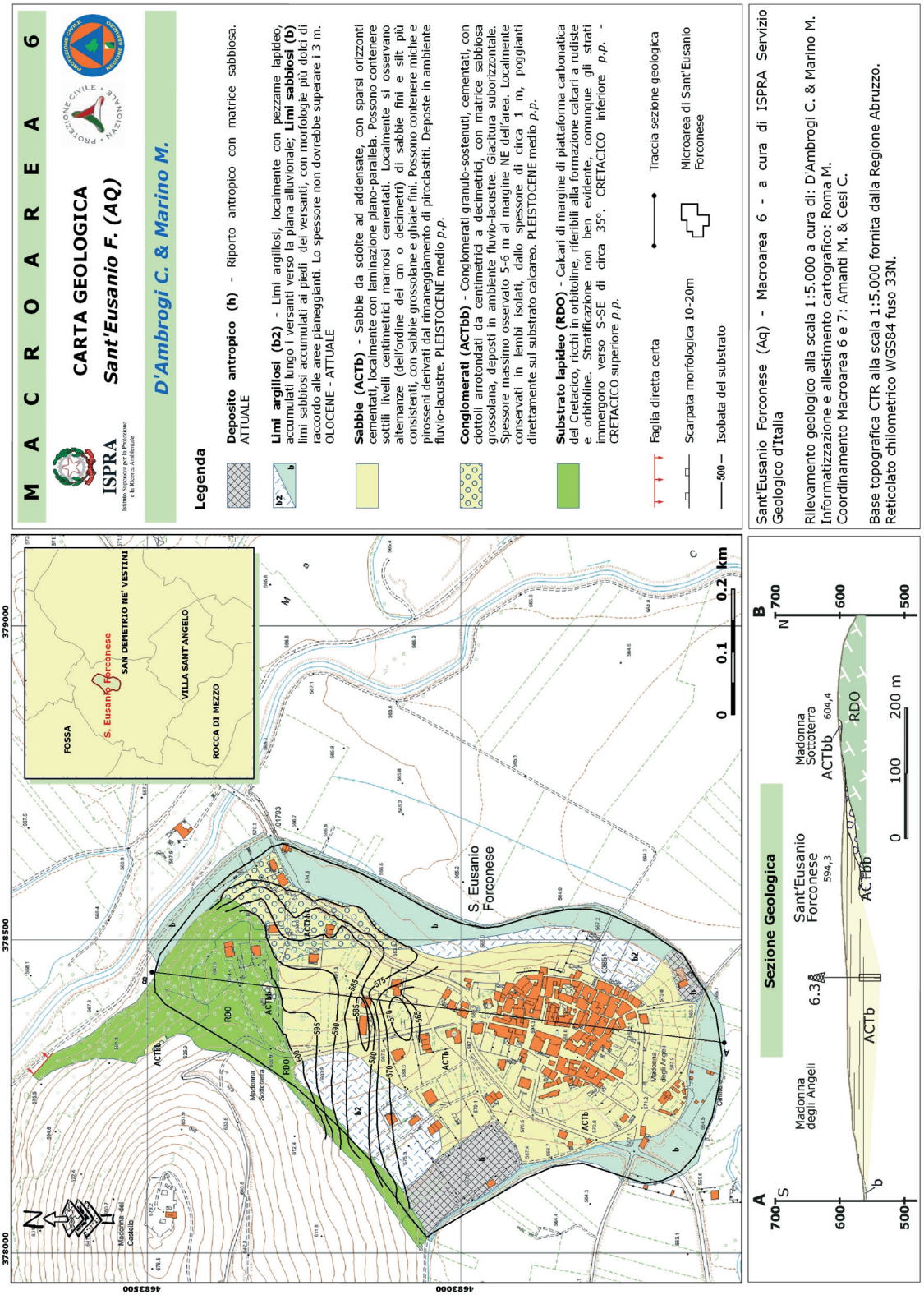

Fig. 7 - Geological map of Sant'Eusanio Forconese.

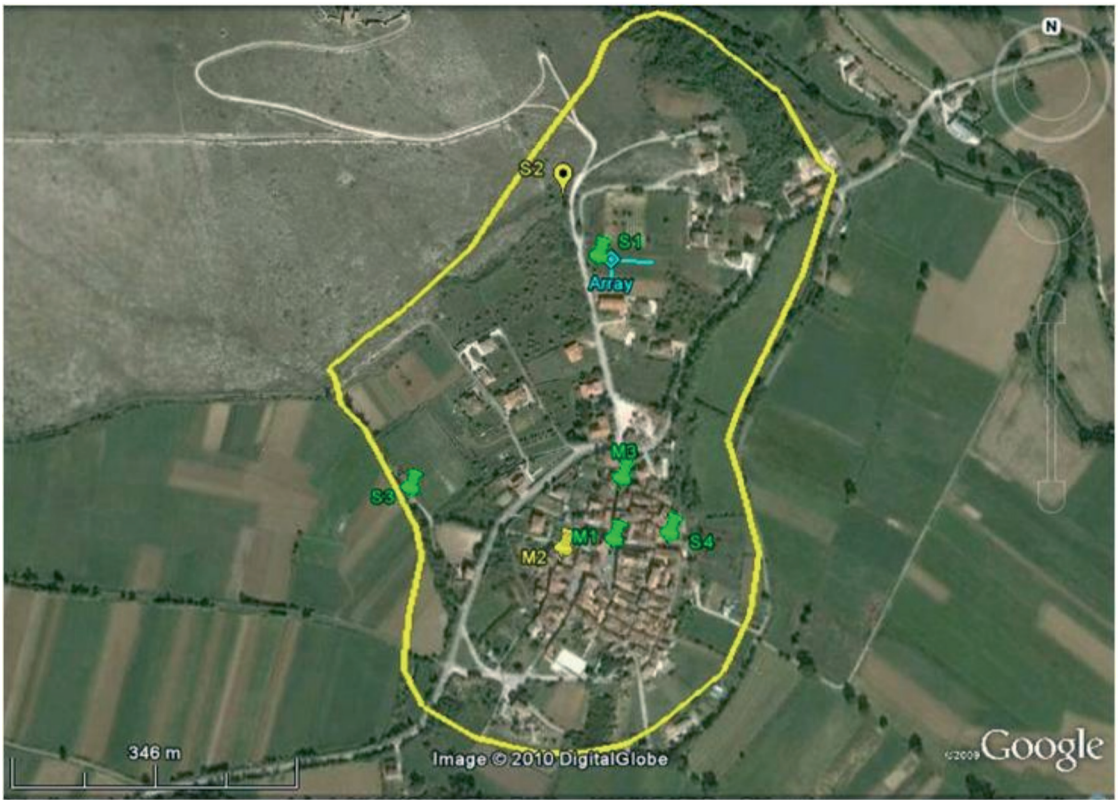

Fig. 8 - Distribution of the passive measurements (both single- and multi-station) effectuated in the area of Sant'Eusanio Forconese. The colors refer to single-station measurement quality (green: class A; yellow: class B), where the two symbols indicate the presence or not of a peak (drawing pin: type 1, i.e., presence of at least a pick; drop: type 2, i.e., no pick). The array branches are pointed out by two cyan segments.

fracturing. In other places, the resonance effect is due to the contrast between a soft cover and underlying stiff materials that do not correspond to the geological substratum: sites of San Demetrio nei Vestini (c, d in Fig. 4) and Stiffe (f in Fig. 4). In the site of Vallecupa (g in Fig. 4), data are insuffcient to establish seismic properties of materials below the interface, but the other kind of surveys allow us to identify it as the geological substratum. It is interesting to observe the existence, in many cases, of two resonant interfaces.

In order to show an application of the procedure described above, results obtained at the settlement of Sant'Eusanio Forconese, included into the macroarea 6, are discussed in detail in the next subsection.

5.2. An example of integrated study: Sant'Eusanio Forconese

Fig. 6 shows the distribution of geophysical measurements carried on in the area.

The area is characterized by the outcropping of a thick sedimentary succession (belonging to the Laziale-Abruzzese platform succession) gently dipping to the south (Fig. 7). In unconformities above this last, a thin conglomerate sequence was recognized, characterized by etherometric and well rounded pebbles. These conglomerates were linked to continental

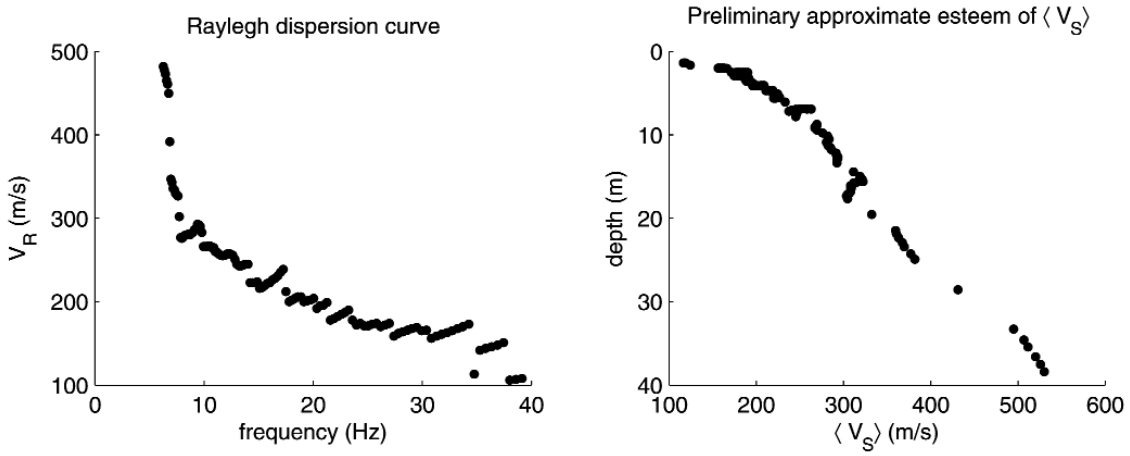

Fig. 9 - A "fast and dirty" inversion by dispersion curve at site of Sant'Eusanio Forconese. Left: experimental V_R curve. Right: approximate pattern of average S-wave velocity profile obtained by Eq. (6).

processes, mainly fluvial-lacustrine. The whole area is also characterized by a widespread outcropping of a thick sandy fluvio-lacustrine deposit and pebbly-sandy alluvial deposits. From a structural point of view the area is characterized by the Cretaceous sedimentary succession gently dipping to the south, while the northern edge of the carbonatic ridge is highlighted by an important NE dipping normal fault. The field analyses carried out allow us to define this fault system as an Apenninic lineament NW-SE trending with a height dip angle comprised between 70° to 80°. The fault system offsets the whole sedimentary succession to the NE downwards. The geological cross-section highlighted the relationships between the continental cover and the carbonatic substratum. The section trace was realized to emphasize the close geometrical and stratigraphic relationships between the different lithological sequences recognized. Despite this no fault were intercepted within the cross section.

As a whole, 7 single-station measurements (HVSR) were executed: 5 of them resulted in class A and the residual 2 in class B (Fig. 8). A passive seismic array was also provided to constrain the shear wave velocity profile in the subsoil. To this purpose, a suitable location was identified in the north of the hamlet (Fig. 8). The obtained V_R curve is shown in Fig. 9, along the relative approximate inversion performed by Eq. (6). The single-station measurements M1, M2, M3, S1, S4 resulted directly interpretable (they are in class A, except M2 that is in class B) and presented a very sharp maximum in the HVSR curve in correspondence of frequencies that increase from 2.5 to 3 Hz moving northwards: this suggested a smooth uprising of the resonant surface in this direction. The high values of the HVSR peaks point out the presence of a strong impedance contrast in correspondence of this surface. The very preliminary interpretation provided by correspondences in Table 1, suggested a thickness of this layer in the range 30 ÷ 50 m. By taking into account an average S-wave velocity in the soft sedimentary cover of the order of 400÷500 m/s ($\langle V_S \rangle$ profile in Fig. 9), the estimated depth of this interface is confirmed. Measurement S3 (of class A type 1) shows a sharp maximum at 3 Hz, with a high value of the H/V ratio. This fairly matches with the fact that the place of this measurement seems to lie on a filling material with a

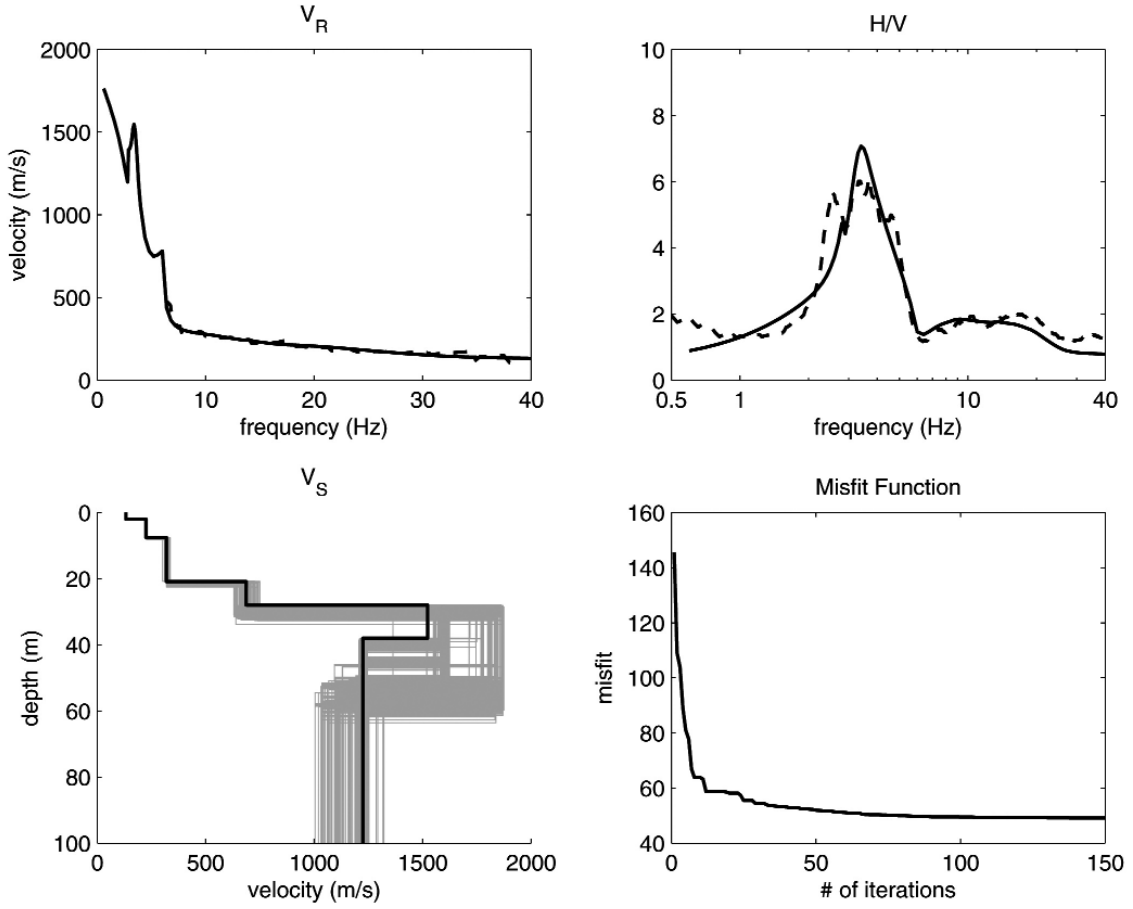

Fig. 10 - Joint inversion results of the effective dispersion curve and the HVSR curve, obtained in the same place, at site of Sant'Eusanio Forconese. Top left: comparison of theoretical dispersion curve resulting from the inversion (solid line) and the experimental ones (dashed line). Top right: comparison of theoretical HVSR curve (solid line) and the experimental ones (dashed line). Bottom left: the S-wave velocity profile of the best-fit model (black line) with (grey lines) the velocity values of the profile with a misfit function value not higher than the 10% of the one of the best-fit model. Bottom right: the best misfit function pattern.

thickness of about 20 m, as it has been computed estimating the S-wave velocity near to 200 ÷ 300 m/s. Finally, the measurement S2 did not show clear maxima. This confirms the role of the bedrock for outcrops where this measuring site is located (RDO in Fig. 7).

The dispersion curve deduced from the array measurement was inverted jointly with the HVSR curve obtained nearby (S1) with the genetic algorithm method. The resulting profile shows a variation of the shear wave velocity from about 300 to more than 1200 m/s around 25 m of depth (Fig. 10 and Table 2): probably this transition corresponds to the carbonatic substratum, which outcrops not far (few tens of metres) from the site. The velocity values obtained from this inversion resulted compatible with the ones provided by the down-hole test, executed about 300 m from the array site (see Fig. 6); they are synthesized in Fig. 11. We remark that, by considering its rough character, the values obtained by the "fast and dirty" method are a satisfactory

Table 2 - S-wave velocity profile in array place (Fig. 8). The values correspond to the model which better fits the experimental curves (Fig. 10): h indicates the thickness, where V_S indicate the S-wave velocity.

h (m)	V_S (m/s)
2	132
6	225
13	319
7	687
10	1523
134	1225
∞	2006

approximation of the ones shown in Fig. 10 and Table 2.

In the same area, ISPRA realized a ERT profile along direction SSE-NNW (see Fig. 6). This line extends from the sandy deposits up to the carbonatic substratum. The results of this survey (Fig. 12) show a resistivity increase at depth roughly ranging between 20 and 30 m. Below this zone, the resistivity values are the same as the ones corresponding to the outcropping carbonatic substratum, crossed by the ERT line on the NNW side. According to the seismic survey, the resistivity surface approximately corresponds to the limit between sands and carbonatic substratum, ergo confirms the interpretation of ambient vibration results described above.

6. Conclusions

The seismic microzonig project carried on in the area shaken by the April 6, 2009 L'Aquila earthquake [whose global results will be published in Gruppo di Lavoro MS L'Aquila (2011)] was characterized by three peculiarities: a relatively large dimension of the investigated area (of the order of 10^3 km^2), the very little time available to provide results (2 ÷ 4 months for the whole set of activities), cooperation of a heterogeneous group of researchers (geologists, geophysicists, geotechnical engineers), including public research institutions, local administrations and professional subjects. In this frame, the application of fast, cost effective and easy-to-use exploratory tools was mandatory. For this purpose, ambient vibration monitoring (both in single-station and multi-station configurations) represented an effective solution. Single-station acquisitions were widely applied allowing large areas to be surveyed by few operators working in parallel. Furthermore, due to the very low soil occupancy necessary for these kinds of measurements, these were effectively used in strongly anthropized areas where the presence of buildings and narrow streets prevented the use of other prospecting techniques. To better constrain the local V_S profile, ambient vibration measurements were also provided with arrays of vertical geophones, managed by a small number of operators (2 ÷ 3 operating within a couple of hours from each measurement). Thus, by using this kind of passive prospecting techniques, it was possible to explore a small settlement in about half a day by a small group of operators (3 ÷ 4). In this way, in the months following the earthquake, relatively broad areas were explored without any significant limitation related to the level of anthropization and damages.

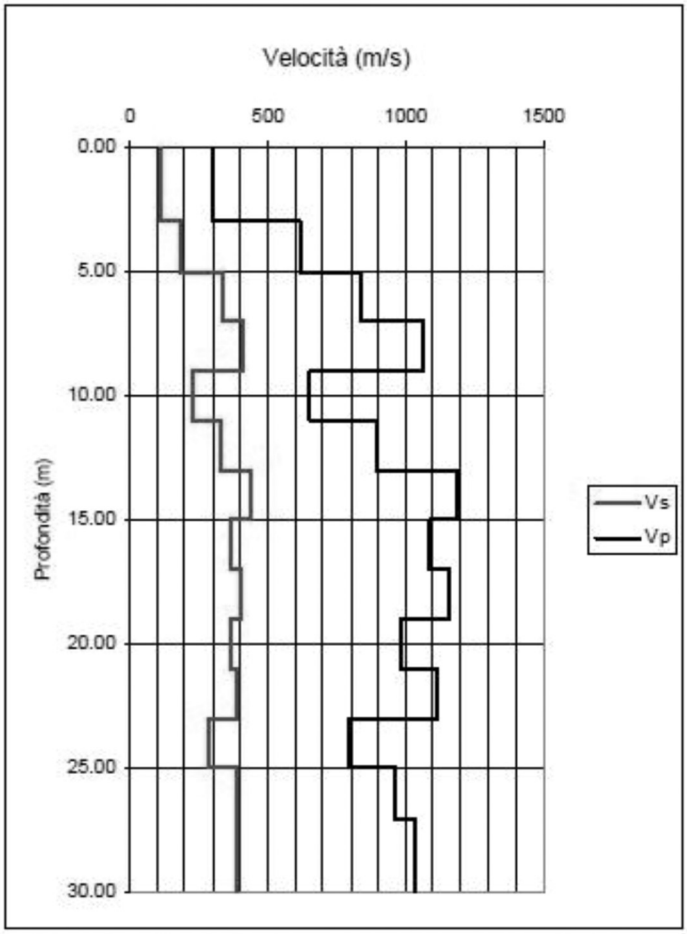

Profondità	Vp	Vs	Vp/Vs	Poisson
1.00	296	111	2.67	0.42
3.00	617	182	3.40	0.45
5.00	833	336	2.48	0.40
7.00	1064	411	2.59	0.41
9.00	652	226	2.89	0.43
11.00	895	327	2.74	0.42
13.00	1194	439	2.72	0.42
15.00	1084	364	2.98	0.44
17.00	1158	402	2.88	0.43
19.00	981	360	2.72	0.42
21.00	1114	389	2.86	0.43
23.00	797	281	2.84	0.43
25.00	962	390	2.47	0.40
27.00	1032	390	2.64	0.42

Fig. 11 - Down-hole test results at Sant'Eusanio Forconese: *velocità*=velocity, *profondità*=depth, *Poisson*= Possoin's ratio. Depth values are in m and velocity ones are in m/s.

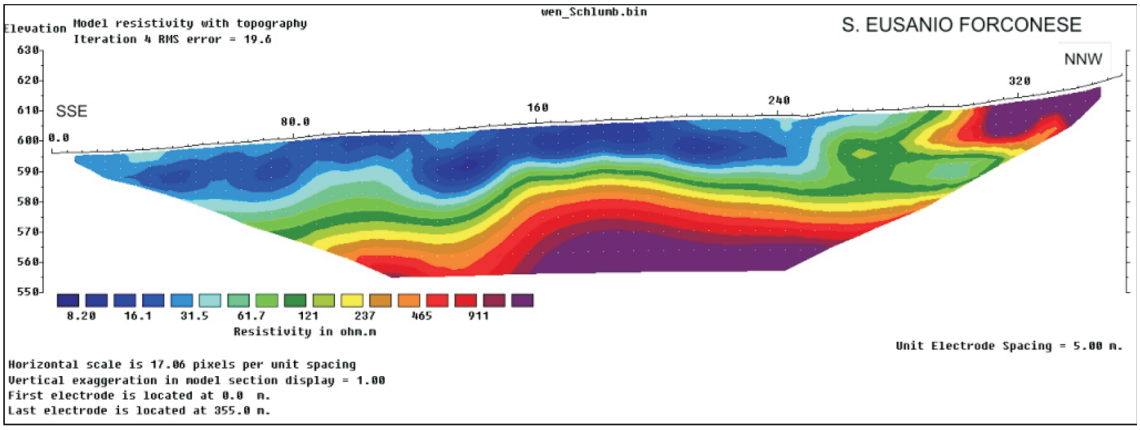

Fig. 12 - Geoectrical tomography (ERT) in the area of Sant'Eusanio Forconese.

Single-station measurements were processed by following the HVSR approach to identify sites where possible seismic resonance effects took place and to measure the relevant resonance frequencies f_0. These pieces of information were used to provide a nearly real-time evaluation (very preliminary) of the seismic bedrock pattern and revealed to be very useful in supporting geological prospecting, aiming at the definition of the preliminary geological model of the areas under study.

Multi-station measurements were processed by using the ESAC approach to evaluate the effective (or apparent) Rayleigh waves dispersion curve. This was used to constrain the local V_S profiles by a joint inversion procedure that fully exploited single-station and array ambient vibration measurements carried out at the same site. It is worth noting that V_S values provided in this way reached depths that in many cases exceeded those actually attainable by drillings (mostly limited below a 40 m depth in the study area) and conventional seismic surveys. In the light of these last results, preliminary interpretation of distributed HVSR data were revised to provide more reliable evaluations of the bedrock depths. In fact, availability of such refined interpretation and of distributed f_0 estimates, along with results of geological surveys, allowed us to extend the results obtained beneath the array to the surrounding areas. The possibility of such lateral extrapolation also concerns results provided by other techniques, such as down-hole tests or active seismic measurements.

Results obtained from these analyses were compared with results provided by geological surveys and geophysical prospecting. This allowed a re-interpretation of V_S profiles and buried morphologies revealed by passive seismic surveys. Furthermore, this provided an extensive test of ambient vibration monitoring as an effective tool for seismic microzoning. As a result of this test, a tentative protocol can be defined as a guideline for the use of passive seismic surveys in microzoning little villages or similar areas, especially in case of urgency.

In primis, some very rough indication about local geology of areas of interest is very important to define the correct distribution of single-station measuring sites. A first survey of single station measurements accompanied by preliminary data processing and interpretation turn

out to be very important to drive geological prospecting and to better plan future subsequent geophysical measurements. In order to better constrain the local V_S profile, at least one multi-station (array) measurement has to be carried out in the most interesting zone (e.g., the hamlet) along with a single-station measurement to be realized in the same position. These data can feed suitable joint-inversion procedures, eventually constrained by independent information available in the area (resistivity prospecting, in-hole measurements, etc.), to define the local V_S profile. In this phase, availability of distributed measurements allows the lateral prolongation of point-like dynamical parameterization of the shallow subsoil and the development of effective numerical models to estimate the seismic response in the whole study area.

REFERENCES

Albarello D. and Gargani F.; 2010: *Providing NEHRP soil classification from the direct interpretation of effective Rayleigh waves dispersion curves.* Bull. Seismol. Soc. Am., **100**, 3284–3294, doi: 10.1785/0120100052.

Albarello D. and Lunedei E.; 2010: *Alternative interpretations of horizontal to vertical spectral ratios of ambient vibrations: new insights from theoretical modeling.* Bull. Earthq. Eng., **8,** 519–534, doi: 10.1007/s10518-009-9110-0.

Arai H. and Tokimatsu K.; 2004: *S-wave velocity profiling by inversion of microtremor H/V spectrum.* Bull. Seism. Soc. Am., **94**, 53–63.

Arai H. and Tokimatsu K.; 2005: *S-wave velocity profiling by joint inversion of microtremor dispersion curve and horizontal-to-vertical (H/V) spectrum.* Bull. Seismol. Soc. Am., **95**, 1766-1778.

Bonnefoy-Claudet S., Cornou C., Bard P.Y., Cotton F., Moczo P., Kristek J. and Fäh D.; 2006: *H/V ratio: a tool for site effects evaluation. Results from 1-D noise simulations.* Geophys. J. Int., **167**, 827–837.

Chandler A.M., Lam N.T.K. and Tsang H.H.; 2005: *Shear wave velocity modelling in crustal rock for seismic hazard analysis.* Soil Dyn. Earthq. Eng., **25**, 167–185.

D'Amico V., Albarello D., Baliva F., Picozzi M. and Agili F.; 2006a: *Site response characterization of the Florence urban area (Italy) using seismic noise measurements.* In: 1st European Conference on Earthquake Engineering and Seismology, Geneva, Switzerland, Abstract Book, pp. 333.

D'Amico V., Picozzi M., Albarello D., Naso G. and Tropenscovino S.; 2004: *Quick estimates of soft sediment thicknesses from ambient noise horizontal to vertical spectral ratios: a case study in southern Italy.* J. Earthq. Eng., **8**, 895–908.

D'Amico V., Picozzi M., Baliva F. and Albarello D.; 2008: *Ambient noise measurements for preliminary site-effects characterization in the urban area of Florence.* Bull. Seismol. Soc. Am., **98**, 1373-1388, doi: 10.1785/0120070231.

D'Amico V., Picozzi M., Baliva F., Albarello D., Menichetti M., Bozzano F., Martino S., Rivellino S. and Scarascia Mugnozza G.; 2006b: *Test sites in Europe for the evaluation of ground motion amplification: site response of the Gubbio basin (central Italy) using geological data and seismic noise measurements*. In: 1st European Conference on Earthquake Engineering and Seismology, Geneva, Switzerland, Abstract Book, pp. 301.

Delgado J., Lopez Casado C., Estevez A., Giner J., Cuenca A. and Molina S.; 2000a: *Mapping soft soils in the Segura river valley (SE Spain): a case study of microtremors as an exploration tool.* J. Appl. Geophys., **45**, 19–32.

Delgado J., Lopez Casado C., Giner J., Estevez A., Cuenca A. and Molina S.; 2000b: *Microtremors as a geophysical exploration tool: applications and limitations*. Pure Appl. Geophys., **157**, 1445–1462.

DPC; 2009: *La microzonazione sismica dell'area aquilana.* <http://www.protezionecivile.it/cms/view.php?dir_pk=395&cms_pk=17356>.

Fäh D., Kind F. and Giardini D.; 2001: *A theoretical investigation of average H/V ratios.* Geophys. J. Int., **145**, 535-549.

Faust LY.; 1951: *Seismic velocity as a function of depth and geologic time.* Geophysics, **16**, 192–206.

Forbriger T.; 2006: *Low-frequency limit for H/V studies due to tilt.* Sitzung der Arbeitsgruppe Seismologie des FKPE. Haidhof, Germany, Extended Abstract, **32**.

Gruppo di Lavoro MS; 2008: *Indirizzi e criteri per la microzonazione sismica. Conferenza delle Regioni e delle Province autonome.* Dipartimento della Protezione Civile, Roma, 3 vol. e 1 DVD.

Gruppo di Lavoro MS L'Aquila; 2011: *La microzonazione sismica per la ricostruzione dell'area aquilana*. Dipartimento

della Protezione Civile - Regione Abruzzo, 3 vol. e 1 DVD, in press.

Hinzen K.G., Scherbaum F. and Weber B.; 2004: *On the resolution of H/V measurements to determinesediment thickness, a case study across a normal fault in the Lower Rhine embayment, Germany*. J. Earthq. Eng., **8**, 909–926.

Ibs Von Seht M. and Wohlemberg J.; 1999: *Microtremor measurements used to map thickness of soft sediments.* Bull. Seismol. Soc. Am., **89**, 250–259.

Konno K. and Kataoka S.; 2000: *An estimating method for the average S-wave velocity of ground from the phase velocity of Rayleigh wave.* Proceedings of JSCE., **647**, 415–423.

Lunedei E. and Albarello D.; 2009: *On the seismic noise wavefield in a weakly dissipative layered. Earth.* Geophys. J. Int., **177**, 1001-1014, doi: 10.1111/j.1365-246X.2008.04062.x.

Lunedei E. and Albarello D.; 2010: *Theoretical HVSR curves from full wavefield modelling of ambient vibrations in a weakly dissipative layered. Earth.* Geophys. J. Int., **181**, 1093-1108, doi: 10.1111/j.1365-246X.2010.04560.x.

Martin A.J. and Diehl J.G.; 2004*: Practical experience using a simplified procedure to measure average shear wave velocity to a depth of 30 meters (VS30)*. In: 13th World Conference on Earthquake Engineering, Vancouver, B.C., Canada, August 1–6, 2004, paper n. 952.

Menke W.; 1989: *Geophysical data analysis: discrete inverse theory*. Academic Press Inc., San Diego California USA, 289 pp.

Nakamura Y.; 1989: *A method for dynamic characteristics estimation of subsurface using microtremor on the ground surface.* Quarterly Report Railway Tech. Res. Inst., **30**, 25–30.

Nakamura Y.; 2000: *Clear identification of fundamental idea of Nakamura's technique and its applications.* In: Proceedings of the 12th World Conference on Earthquake Engineering, Auckland, New Zealand, note 2656.

Ohori M., Nobata A. and Wakamatsu K.; 2002: *A comparison of ESAC and Fk methods of estimating phase velocity using arbitrarily shaped micritremor arrays.* Bull. Seism. Soc. Am., **92**, 2323-2332.

Okada H.; 2003: *The microtremor survey method.* Geophysical Monograph Series, SEG, 129 pp.

Parolai S., Bormann P. and Milkereit C.; 2002: *New relationships between Vs, thickness of sediments and resonance frequency calculated from H/V ratio of seismic noise for the Cologne area.* Bull. Seismol. Soc. Am., **92**, 2521–2527.

Parolai S., Picozzi M., Richwalski S.M. and Milkereit C.; 2005: *Joint inversion of phase velocity dispersion and H/V ratio curves from seismic noise recordings using a genetic algorithm, considering higher modes*. Geophys. Res. Lett., **32**, L01303, doi: 10.1029/2004GL021115.

Parolai S., Richwalski S.M., Milkereit C. and Faeh D.; 2006: *S-wave velocity profile for earthquake engineering purposes for the Cologne area (Germany).* Bull. Earthquake Eng., **4**, 65-94, doi: 10.1007/s10518-005-5758-2.

Picozzi M. and Albarello D.; 2007: *Combining genetic and linearized algorithms for a two-step joint inversion of Rayleigh wave dispersion and H/V spectral ratio curves.* Geophys. J. Int., **169**, 189-200.

Picozzi M., Parolai S. and Richwalski S.M.; 2005: *Joint inversion of H/V ratios and dispersion curves from seismic noise: estimating the S-wave velocity of bedrock.* Geophys. Res. Lett., **32**, L11308, doi: 10.1029/2005GL022878.

Sambridge M. and Mosegaard K.; 2002: *Monte Carlo methods in geophysical inverse problems.* Review of Geophysics, **40**, 1–27.

Scherbaum F., Hinzen K.G. and Ohrnberger M.; 2003: *Determination of shallow shearwave velocity profiles in Cologne, Germany area using ambient vibrations.* Geophys. J. Int., **152**, 597–612.

Sheriff R.E. and Geldart L.P.; 1995: *Exploration seismology.* Cambridge un. Press, Cambridge MA, 592 pp.

SESAME; 2004: *Guidelines for the implementation of the H/V spectral ratio technique on ambient vibrations.* SESAME, European project, WP12, Deliverable D23.12, <http://sesame-fp5.obs.ujf-grenoble.fr/SES_TechnicalDoc.htm>.

SESAME; 2005: *Final report WP13: recommendations for quality array measurements and processing*. SESAME, European project, WP13, Deliverable D24.13, <http://sesame-fp5.obs.ujf-grenoble.fr/SES_TechnicalDoc.htm>.

Tokimatsu K.; 1997: *Geotechnical site characterization using surface waves.* In: Ishihara K. (ed), Proc. 1st Intl. Conf. Earthquake Geotechnical Engeneering, A.A. Balkema, Brookfield VT, pp. 1333–1368.

Xia J., Miller R.D. and Park C.B.; 1999: *Estimation of near surface shear wave velocity by inversion of Rayleigh waves*. Geophysics, **64**, 691–700.

Yamanaka H. and Ishida H.; 1996: *Application of GENETIC algorithms to an inversion of surface-wave dispersion data.* Bull. Seismol. Soc. Am., **86**, 436-444.

Appendix

On average, the mean body-wave velocity in a stratum of recent sediments grown with depth. In general this is an effect of the sediment compaction due to the lithostatic load. On the basis of experimental data, Faust (1951) proposed a generic non-linear relationship between the P-wave velocity (V_P) and the depth Z as

$$V_P(Z) = k \cdot (Za)^{\frac{1}{6}}. \tag{A1}$$

As foundation of this formula theoretical arguments have been supplied (Sheriff and Geldart, 1995) under the hypothesis that the sediment can be imagined as a system of elastic spheres subjected to compression due to the lithostatic load. Eq. (A1) can be written in the more general form:

$$V_P(Z) = V_{P,Z_0} \cdot \left(\frac{Z}{Z_0} \right)^{\frac{1}{6}}, \tag{A2}$$

where V_{PZ_0} is the P-wave velocity at the reference depth Z_0.

On the base of a number of experimental studies concerning shallow sedimentary structures (Z < 4 km) in several world areas, Chandler *et al.* (2005) stated an empirical relationship that allows one to define the value of the mean ratio between V_P values and the correspondent S-wave velocity values (V_S) as a function of the depth Z, which has the form:

$$\frac{V_S(Z)}{V_P(Z)} \simeq 0.58 \cdot \left(\frac{Z}{4} \right)^{\frac{1}{12}}, \tag{A3}$$

where Z is in metres.

By blending Eqs. (A2) and (A3) we obtain the formula:

$$V_S(Z) \simeq V_{S,Z_0} \cdot \left(\frac{Z}{Z_0} \right)^{\frac{1}{4}}, \tag{A4}$$

which represents the average pattern of the S-wave velocity as a function of the depth. By assuming that Z_0 = 1 m and by calling V_0 the S-wave velocity at the depth of 1 m, last formula becomes

$$V_S(Z) \simeq V_0 \cdot Z^{\frac{1}{4}}, \tag{A5}$$

which holds for each dimensionless depth parameter $Z \geq 1$. As we put $z \equiv Z - 1$ (so that the depth is measured starting from 1 m), we obtain

$$V_S(z) \simeq V_0 \cdot (1+z)^{\frac{1}{4}}, \tag{A6}$$

where $V_S(z)$ is the S-wave velocity of the depth $(1+z)\cdot 1$ m. Strictly speaking, this formula holds for granular media only, i.e., for media such as sands. In real cases, saturation level, fluid pressure and cementation (besides variations in form of sedimentation or exhumation) can significantly affect the exponent, which controls the dependence of V_S on the depth. In order to take into account these different situations, the last formula can be generalized in the form:

$$V_S(z) \simeq V_0 \cdot (1+z)^x, \tag{A7}$$

with $x \in]0, 1[$, which holds for each (dimensionless) $z \geq 0$. Experimental results obtained in different sedimentary environments (Ibs von Seth and Wohlenberg, 1999; Delgado *et al*., 2000a, 2000b; Parolai *et al*., 2002; Scherbaum *et al*., 2003; Hinzen *et al*., 2004; D'Amico *et al*., 2006a, 2006b) suggest that:

1) granular soils (sands) present values of x near to 0.25;
2) lower values of x should correspond to fine soils (clays and mud), since in these cases the dominant effect is the electrostatic interaction among the particles, which results in a minor effect of the lithostatic load on the form of interaction among them;
3) greater values of x can be expected in rework soils (landslides) or in fan zones with big non-cemented clasts;
4) fluids under pressure can reduce the effect of the lithostatic load, decreasing the exponent x also in granular grounds.

Furthermore, experimental data show that a significant negative correlation exists between the values of V_0 and x: the stronger the lithostatic load effect (i.e., as x is higher), the lower is the expected value of V_S at surface. A tentative parameterization of this correlation can lead to three indicative couples:

- $V_0 \simeq 210$ m/s and $x \simeq 0.20$ for compact soils,
- $V_0 \simeq 170$ m/s and $x \simeq 0.25$ for sands,
- $V_0 \simeq 110$ m/s and $x \simeq 0.40$ for rework or very recent soils.

It is worth noting, however, that, when introduced in Eqs. (A7) and (3), these parameterizations result in very similar thickness estimates (shown in Table 1) for f_0 values in the range $1 \div 20$ Hz, relevant for the present study. This implies that these parameterizations are nearly equivalent in the limit of the applications here considered.

Corresponding author: Dario Albarello
Dipartimento di Scienze della Terra, Università degli Studi di Siena
Via Laterina 8, 53100 Siena, Italy
Phone: +39 0577 233825; fax: +39 0577 233840; e-mail: albarello@unisi.it